RSC Advances

THERMALLY ROBUST CORE SHELL MATERIAL FOR AUTOMOTIVE 3 WAY CATALYSIS HAVING OXYGEN STORAGE CAPACITY

Journal:	*RSC Advances*
Manuscript ID:	RA-ART-04-2015-006989.R1
Article Type:	Paper
Date Submitted by the Author:	14-May-2015
Complete List of Authors:	Stamm Masias, Kimber; Toyota Technical Center, Materials Research Peck, Torin; Toyota Technical Center, Materials Research Fanson, Paul; Toyota Technical Center, Materials Research

Journal Name

ARTICLE

THERMALLY ROBUST CORE-SHELL MATERIAL FOR AUTOMOTIVE 3-WAY CATALYSIS HAVING OXYGEN STORAGE CAPACITY

Received 00th January 20xx,
Accepted 00th January 20xx

DOI: 10.1039/x0xx00000x

www.rsc.org/

K. L. Stamm Masias,[a] T. C. Peck[a] and P. T. Fanson[a]

Herein is reported a method to encapsulate a catalytically active precious metal core with a shell having not only thermal stability, but also oxygen storage. The synthesis is straightforward and carried out in an aqueous system. The shell provides thermal resistance to metal sintering. A multi-metal oxide shell prevents sintering above 1000 °C and imparts oxygen storage to the system. Porosity within the shell allows for gas egress allowing the reactants to reach the catalytic core and products to diffuse away.

Introduction

The The use of platinum group metals as automotive exhaust catalysts to mitigate emissions of unburned hydrocarbons (HC), carbon monoxide (CO) and nitrous oxides (NO_x) is well established.[1] The ability of these metals to oxidize and reduce pollutants is unparalleled by base metal catalysts. A challenge when applying these metal catalysts to automotive exhaust is the temperature of the gas flow causes the catalytic metal nanoparticle to grow over time. This results in a decrease of metal surface area available for catalysis and a limited lifetime for the materials.

Several strategies to mitigate this sintering have been explored, including in-situ redispersion of the precious metal onto the support material. One strategy involves the use of a Pd-containing La-, Fe-, and Co-based perovskite (i.e. the so-called "intelligent catalyst").[2, 3] A second strategy involves Pt nanoparticles deposited onto a strongly interacting support such as cerium-zirconium oxide.[4] In both cases, real time observation of the precious metal did show atmosphere had a large impact on redispersion of the metal nanoparticle.[5] Under oxidizing conditions a metal oxide was formed and due to the strong interaction between the precious metal oxide and the oxide based support a redistribution of the precious metal was observed. Upon cycling the material back to a reducing atmosphere, the oxidized precious metal was reduced to the catalytically active metallic state. However, precise control of reaction conditions requires very precise engine tuning which may affect the performance of the vehicle itself. In addition, these methods are generally less effective at high temperatures which are encountered in automotive applications.

Another method to suppress sintering is to encapsulate the precious metals in a thermally resistant material. One method for precious metal encapsulation is to form a thermally stable barrier around the catalyst particle. Silica overcoating of titania supported Pt particles has shown to limit sintering and exhibit improvement in liquid phase reactions.[6] The complexity of creating the sample, the challenges in limiting the shell thickness, the increase in total volume of an additional inactive component, and creating a barrier material which allows reactants to rapidly diffuse to the catalyst detract from its usefulness for automotive exhaust applications. Atomic Layer Deposition has also been employed to coat catalytically active particles with thermally resistant alumina and silica and offers more control over the thickness and uniformity of the thermal barrier.[7-9] While these materials imparted thermal stability, the questionable gas permeability or lack of inherent shell porosity has been shown to impact diffusion rates for both reactants and products. Additionally, this method is not suitable for large scale production at this time due to the complexity of the method and use of exotic and air-sensitive precursors. Early work to precisely control formation of a thermally resistant layer around a single catalytic particle examined titania-encapsulated metals such as gold.[10] These materials have been synthesized in a non-aqueous medium and tested for CO oxidation activity. The titania shell did impart stability at the temperatures employed for the testing, however, the route to creating the thermal barrier is complicated and requires precise control of condensation of the titania precursor- specifically limiting the synthesis to non-aqueous systems.

Creating a silica shell around a preformed, surfactant-capped Pt particle has reported by Joo et al to be porous enough to

[a] Toyota Technical Center, Ann Arbor, M, USA
† Footnotes relating to the title and/or authors should appear here.
Electronic Supplementary Information (ESI) available: [details of any supplementary information available should be included here]. See DOI: 10.1039/x0xx00000x

allow ethylene to diffuse through the shell, react and diffuse away from the shell.[11] Their report focused on reactions of small molecules, ethylene hydrogenation and CO oxidation, at relatively low temperatures (<400 °C). The activity and thermal stability of the samples was tested in a model system employing a Langmuir-Blodgett film in which the 2-D array itself presents challenges due to the low surface area of the film support and the necessity of increased particle density. While this material shows promise, the sample preparation makes it challenging to argue it could displace traditional production materials in which catalytic materials are deposited on a functional mixed oxide support.

Ceria is well explored in the field of exhaust catalysis as it has the benefit of oxygen storage capacity, wherein labile oxygen which can be donated or adsorbed dependent upon the reaction atmosphere allowing a buffer for non-stoichiometric conditions. The use of ceria to improve catalytic performance is hindered by the need to maximize the contact between ceria and the precious metal catalyst, as well as the thermal instability of pure ceria. A microemulsion approach was used to prepare Pt@CeO_2 for water-gas shift reactions.[12, 13] This work presented a simplistic synthetic method, but the small quantity of product from such a synthetic method limits applicability to industrial production. Cargnello et al have explored the use of sol-gel chemistries employing complex precursors to produce ceria encapsulated palladium for CO oxidation.[14, 15] The ceria encapsulation imparts functionality to a shell and was shown to improve catalytic activity of the material by limiting precious metal sintering. This intimate contact between the ceria and Pd allowed for improved utilization of the oxygen storage capacity. The process involved preforming Pd nanoparticles capped with a polymer, and condensing a ceria alkoxide compound around the particle in an air free environment. While this was an elegant piece of chemistry, the complexity of synthesizing the ceria precursor hinders application of the Pd surrounded by pure ceria.

We present here a new approach which builds on the previous literature by combining the thermal stability seen in other metal oxide shells, nanoscale control of this thermal barrier, the ease of the aqueous synthesis of the silica shell, as well as functionality and proximity of the ceria component to the catalyst. Finally, sample preparation and testing conditions employed in industrial automotive exhaust testing must also be at the forefront of the work. This strategy resulted in a material with improved durability and increased utilization of oxygen storage capacity compared to traditional exhaust catalyst materials.

Experimental

In order to prepare isolated Pt nanoparticles, a 247mL aqueous solution was prepared in a 500mL round bottom flask by heating 0.1M cetyl trimethyl ammonium bromide (CTAB) and 0.001M chloroplatinic acid at 60 °C for 30 minutes or until the solution became clear. To this solution a $NaBH_4$ solution was added drop‐wise to achieve a final $NaBH_4$:Pt ratio of 25:1 in a total of 250 mL. The solution was allowed to stir for 16 hours during which time the color changed from orange to grey. The solution was centrifuged at 4000RPM for 3 minutes to precipitate any large particles, and then at 14,000RPM for 30 minutes, three times, to isolate Pt nanoparticles. The isolated particles were then resuspended in and aqueous system consisting of 0.0035M tetraethyl orthosilicate (TEOS) or 0.008M cerium nitrate/0.0035M TEOS solution and allowed to stir at room temperature 20 minutes. To the stirring solution, 0.05mL NH_4OH and 2.2mL methanol were added, bringing the total volume to 250 mL. The solution continued to stir for 55 hours at which time the particles were precipitated by centrifugation. The solution was exposed to atmosphere throughout the synthesis.

Transmission electron microscopy (TEM) was performed on a Hitachi 9500. The Pt@metal oxide particles described above were suspended in deionized water and deposited dropwise onto a carbon-coated TEM grid for particle size analysis. Details for in-situ thermal analysis have been described elsewhere.[16] Briefly, the suspended particles were brushed onto a tungsten coil filament mounted within the TEM holder. In-situ temperature was correlated by a calibration curve to the current applied to the filament. The current was adjusted over a period of 30 minutes from the initial temperature to the desired temperature and held at the temperature for 30 minutes before acquiring images and continuing to ramp to the next desired temperature. During the temperature ramp, adjustments to sample position and focus were performed as needed to compensate for image drift and expansion of the tungsten filament.

For all other testing, including evaluation of catalytic activity, the particles were deposited onto the external surface of a non‐porous gamma alumina (150 m^2/g) support via wet impregnation such that the weight loading of Pt was controlled to be 0.2-0.5 weight percent. Comparison samples of Pt on the same alumina support were prepared by incipient wetness. A platinum nitrate solution was applied to a commercial ceria-zirconia (60 weight %CeO_2, 30 weight % ZrO_2, 3 weight % La_2O_3, 7 weight % Pr_6O_{11}, 87 m^2/g) and dried under gentle heating on a hot plate prior to calcination. All supported samples were calcined in air for 2 hours at 600 °C, 800 °C, or 1000 °C in order to simulate the aging of the catalyst material. The reference platinum on alumina and platinum on ceria‐zirconia were also prepared at 0.2-0.5 weight percent of platinum.

Elemental composition for each sample was determined by Inductively Coupled Plasma-Optical Emission Spectrometry (ICP-OES, Galbraith Laboratories). For the non-ceria containing materials, the active platinum surface was measured by pulse CO chemisorption employing a Micromeretics 2920. Three-way catalytic activity and oxygen storage capacity were probed in a packed bed reactor employing a space velocity of 20,000 hr^{-1} and a constant gas flow of 140 mL/minute. The total mass of material in the test bed was 500mg using quartz sand as a

dilutant. Samples for total catalytic activity were normalized to contain 0.375mg Pt. The samples were pretreated for one hour at 500 °C in a H_2 atmosphere before exposing the sample to a linear temperature ramp from 50 °C to 600 °C at 10 °C/min employing gas concentrations of 1000 ppm propylene, 6500 ppm carbon monoxide, 1500 ppm nitric oxide, and 7000 ppm of oxygen in a balance of helium carrier gas in order to simulate automotive exhaust gas conditions at atmospheric pressure. Oxygen storage of samples after calcination at 800 °C was probed in the same reactor at 300 °C. Test samples mixed with granular silica were of varying masses (20-150mg of catalyst plus quartz) as needed to obtain noise-free data and yet not saturate the MS detector. A known volume of CO_2 gas was pulsed over the sample to calibrate the Mass Spectrometer response, and then alternating a 15 minute pulse of O_2 to saturate the sample followed by a 10 minute CO pulse while monitoring the CO_2 produced.

Results and discussion

ICP-OES measurements show the atomic ratio of elements in the Pt@Silica sample to be 2:1 Pt:Si, and 4:1:2 Pt:Si:Ce in the Pt@silica*ceria particles. As can be seen in Figure 1, transmission electron microscopy of the unsupported nanoparticles revealed 10.4 ±1.6 nm Pt cores surrounded by 5.5 ±0.8 nm silica shells. When ceria was added to the shell, the size of both the core and shell was essentially unchanged; 10.7 ± 1.2nm Pt surrounded by 6.0 ± 0.8nm silica*ceria shells, (Figure 1). In both cases the particles sizes for each sample were measured using a sample size of n≥30. Energy dispersive spectroscopy of the sample within the TEM column indicated ceria was uniformly distributed in the silica-containing regions. However, the morphology of the shells with the ceria component appears rougher in appearance as compared to the more uniform silica shells. In the case of the ceria containing shell, it is possible small isolated crystallites of the ceria-silica shell material were precipitated independently from the Pt particle, which can be seen in the sample drop cast on the TEM grid.

The thermal stability of the unsupported core-shell nanoparticles was measured using In-situ thermal TEM (See Figure 1). In this case, the geometry of the sample holder allowed for the monitoring of fewer particles (typically 15 per sample), but individual Pt nanoparticles were able to be continuously monitored as a function of temperature from room temperature up to 1100°C. For both the silica and silica-ceria shell nanomaterial, the size of the Pt cores did not appear to change significantly over the course of the heating. In some cases, even the shape of the Pt nanocores was unchanged. This observed stability of the Pt cores over a wide temperature ranges suggests that the encapsulation was successful in drastically reducing the rate of sintering for the encapsulated Pt nanoparticles as compared to traditional catalyst materials.[16, 17] The sample preparation technique eliminates

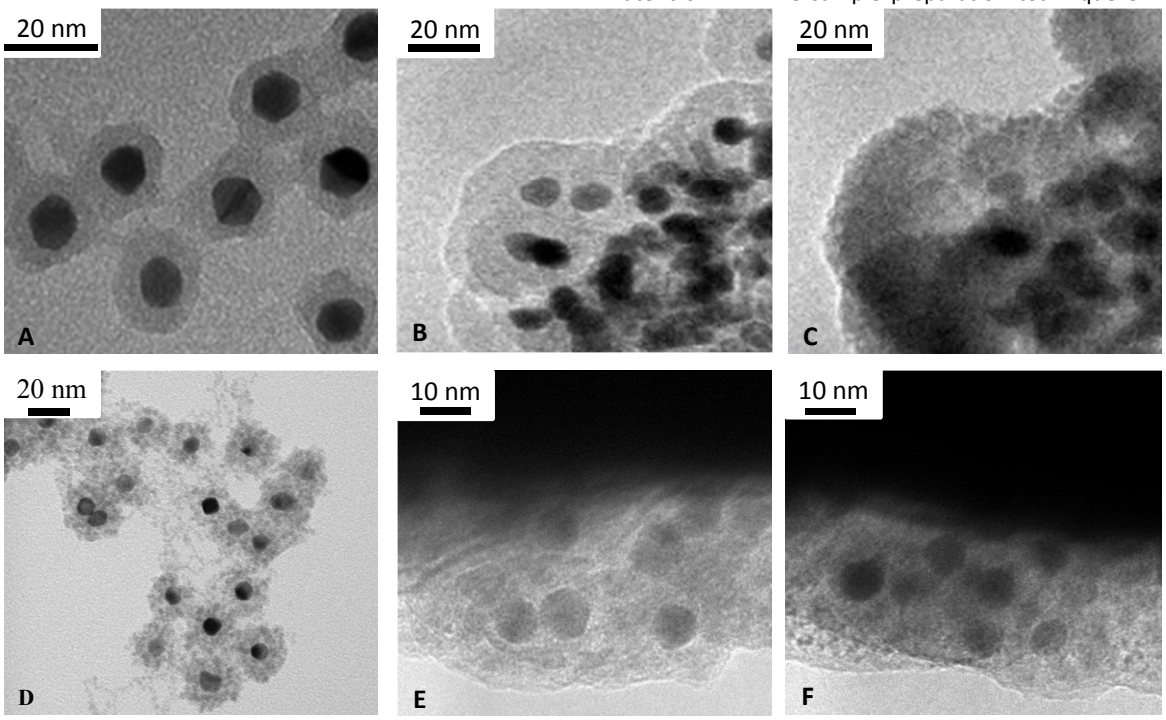

Figure 1. TEM images of (top left to right) Pt@Silica on a carbon grid (A), on a tungsten filament heated under vacuum to 200 °C (B) or 1200 °C (C) and (bottom left to right) Pt@Silica*Ceria on a carbon grid (D), on a tungsten filament heated under vacuum to 200 °C (E), or 1200 °C (F)

the deposition of isolated silica*ceria crystallites as observed on the TEM grid, but these particles may be deposited on top of the encapsulated platinum resulting in a thicker shell. The thermal expansion of the tungsten filament caused sample rotation in the x, y, and z-axes during the observation, making quantitative measurements of the shell more challenging. However, it should be noted that qualitatively, the shell appears more granular after heating. This suggests that for these encapsulated particles, changes in the property of the shell itself may impact the final catalytic properties of the supported catalyst material.

Catalytic testing monitored the conversion of propylene, carbon monoxide, and nitric oxide as a function of temperature. The trends for all gasses were similar and the reported activity of each sample was quantified (see Figure 2) by considering the temperature at which the conversion of propylene (the largest and therefore slowest diffusing molecule) reached 50% (known as the hydrocarbon T-50 temperature, where lower T-50 temperatures indicate higher activity). The reference platinum deposited on alumina material calcined at 600 °C showed a 30 °C lower T-50 temperature than either core@shell sample. While the CTAB surfactant melts below 300 °C, thermal gravitational analysis indicates weight loss continues until after 500 °C, likely due to removal of carbonaceous deposits left from the surfactant decomposition. The porosity created by the surfactant may impede removal of deposits, requiring higher temperatures or longer calcination times. Such pore blockage would also explain the lower catalytic performance of materials calcined at the lower temperature. Additionally, the as-deposited Pt on a commercial support is closer to 3-5nm as opposed to the larger (10 nm) particles for the core@shell materials tested. As can be seen from Figure 2, the T-50 values of the core@shell samples calcined at 800 °C are lower than the reference material, indicating not only that there is sufficient porosity for reactants to reach the core and diffuse out of the shell, but the shell improves overall reactivity. This is most likely due to the ability of the porous ceramic shell to prevent sintering of the active Pt cores. After sintering at 1000 °C, the difference in catalytic activity between the samples is less pronounced, with the ceria doped shell having the lowest light-off temperature. In comparison to the samples aged at 800°C, the ceria doped shell shows almost no degradation in activity, while the silica only shell loses the most activity. Due to the low loading of the material onto the alumina support, pore volume measurements were identical to the support itself, and not able to discern if the change in activity is due to a loss in porosity and therefore gas egress.

Additional insight into the changes in catalyst activity as a function of aging can be gained by examining the results of CO pulse chemisorption on the Pt@silica and Pt on alumina samples (see Figure 3). As expected, the initial particle size for the Pt/Al_2O_3 reference catalyst was measured to be 3.2 nm. In contrast, the Pt particle size for the supported core-shell material was measured to be 36.4 nm. This value is approximately 3x larger than the particle size measured by TEM, which suggests that the ceramic encapsulation and residual surfactant may block up to 90% of the active sites. After aging at 800°C, the CO chemisorption results indicate the growth of the uncoated Pt particles to 45.7 nm. Such growth is commensurate with TEM observations and other published studies of sintering. The particle size of the silica shell material as measured by CO pulse chemisorption is comparable to the uncoated material at 47.5 nm. These changes are qualitatively consistent with the trends observed in the activity study in which the unprotected Pt particles lost significant activity while the activity of the core-shell catalysts remained stable. Upon aging at 1000°C, the unprotected Pt nanoparticles both increase and size as well as decrease in activity. Silica coated Pt particles show little change in size based on pulse CO and TEM measurements, but the activity of the material is not the same as the sample calcined at 800 °C. This decrease in

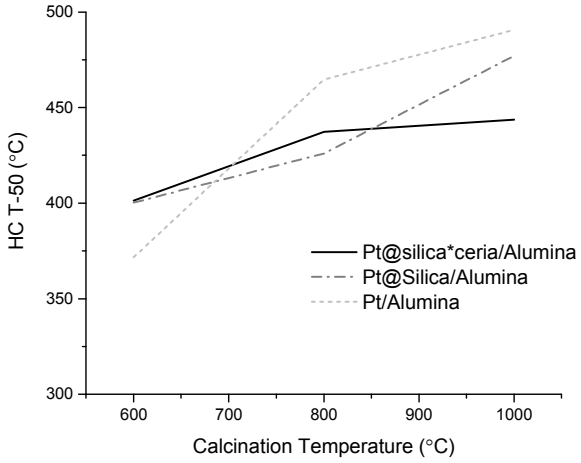

Figure 2. The temperature at which 50% of the hydrocarbon is reacted (T-50) as a function of calcination temperature for Pt on alumina (short dotted line), silica encapsulated platinum on alumina (dash dot line), and platinum encapsulated in a composite of silica and ceria on an alumina support (solid line).

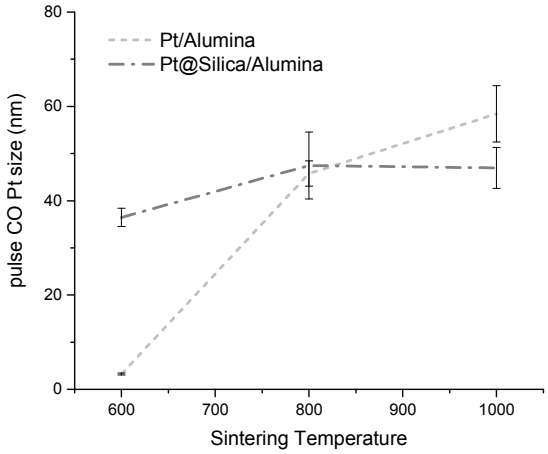

Figure 3. Pulse CO chemisorption measurements of Pt particle diameter as a function of sintering temperature

activity may be related to changes in the pore structure of the silica shell observed in the in-situ TEM.

Measuring Pt size of the ceria-containing samples by pulse CO presented a challenge due to the adsorption of CO onto the ceria and the relatively small amount of Pt in the samples, but TEM analysis suggests the ceria-containing shell limits Pt sintering similar to the silica shell. Interestingly, the activity of the ceria-doped shell nanoparticles exhibited the best performance after aging at 1000°C. The improved stability of these samples may be due to ceria stabilizing the pore structure itself, or it could also be related to potential oxygen storage properties of the ceria-dopant, which will be discussed below.

A step further than the single-phase silica shell, the silica - ceria shell is seen to be similarly thermally robust, but also functional. The oxygen storage capacity of the material was examined by alternating pulses of O_2 and CO at 300 °C. The amount of CO_2 produced by such experiments is correlated to the amount of labile oxygen present in the sample. A simple mass balance assuming CO will reduce Ce^{4+} to Ce^{3+} results in a theoretical maximum of 0.5 moles of CO_2 produced per mole of Ce in the sample. The oxygen storage of the ceria-containing core-shell catalyst was compared to a standard reference catalyst composed of Pt deposited onto a commercial CeO_2-ZrO_2 mixed oxide support at similar Pt loadings, different ceria content. The measured oxygen storage capacity of the core-shell sample is 0.4 moles CO_2 per mole of ceria, within 10% of the theoretical maximum, which suggests that the core-shell nanostructure utilizes the ceria dopant very efficiently. In contrast, the standard reference catalyst utilizes only 0.15 moles of CO_2 per mole of ceria, about 30% of the ceria present in the sample. Similar to previous work, this increase in available oxygen can be attributed to the small size of the ceria shell and the larger fraction exposed to the reactant gasses at the particle surface. This increase of ceria utilization may present an improvement by simply reducing the quantity of this rare earth component of traditional exhaust catalysts and providing oxygen more “on demand” as the proximity of the precious metal and oxygen storage component is necessarily always with a distance of less than 20 nm.

Conclusions

A simple method for creating a thermally robust and functional shell around a catalytically active core in an aqueous system has been presented. Porosity of the shell can be inferred from the gas egress to and from the particle. While sintering of the Pt particle was not observed until well beyond 1000 °C, the porosity is likely reduced, resulting in the still small catalyst particles being less accessible for reaction. Even with any loss in porosity or change in shell structure, the core@shell material outperformed the platinum on alumina reference after sintering. The additional phase within the shell presents an opportunity to improve the utilization of ceria as an oxygen storage material. A further benefit is the reduction of ceria portion of the material when compared to the production materials, allowing a reduction in the usage of the rare earth metals. Application of this method to additional precious metals would likely improve thermal stability for other materials, and improve overall thermal stability of materials within the harsh environment of an automotive exhaust catalyst as well as other applications.

Acknowledgements

The authors would like to thank Charles Campbell, Charles Roberts and Hirohito Hirata for fruitful discussions and valuable insight throughout the course of the work. Thermal TEM images were acquired by Joan Hudson of Clemson University.

Notes and references

1. R. M. Heck and R. J. Farrauto, *Catalytic Air Pollution Control*, John Wiley & Sons, Inc., New York, 2 edn., 2002.
2. Y. Nishihata, J. Mizuki, T. Akao, H. Tanaka, M. Uenishi, M. Kimura, T. Okamoto and N. Hamada, *Nature*, 2002, **418**, 164-167.
3. H. Tanaka, I. Tan, M. Uenishi, M. Kimura and K. Dohmae, *Topics in Catalysis*, 2001, **16**, 63-70.
4. H. Shinjoh, M. Hatanaka, Y. Nagai, T. Tanabe, N. Takahashi, T. Yoshida and Y. Miyake, *Topics in Catalysis*, 2009, **52**, 1967-1971.
5. Y. Nagai, K. Dohmae, Y. Ikeda, N. Takagi, N. Hara, T. Tanabe, G. Guilera, S. Pascarelli, M. A. Newton, N. Takahashi, H. Shinjoh and S. i. Matsumoto, *Catalysis Today*, 2010, **175**, 133-140.
6. K. Yoon, Y. Yang, P. Lu, D. Wan, H.-C. Peng, K. S. Masias, P. T. Fanson, C. T. Campbell and Y. Xia, *Angewandte Chemie International Edition*, 2012, **51**, 9543-9546.
7. J. Lu, J. W. Elam and P. C. Stair, *Accounts of Chemical Research*, 2013, **46**, 1806-1815.
8. J. Lu, B. Liu, J. P. Greeley, Z. Feng, J. A. Libera, Y. Lei, M. J. Bedzyk, P. C. Stair and J. W. Elam, *Chemistry of Materials*, 2012, **24**, 2014-2055.
9. H. Feng, J. Lu, P. C. Stair and J. W. Elam, *Catalysis Letters*, 2011, **141**, 512-517.
10. M. S. Chen Chen, Matteo Cargnello, Paolo Fornasiero, Christopher B. Murray, Raymond J. Gorte, *Catalysis Letters*, 2014, **144**, 1939-1945.
11. S. H. Joo, J. Y. Park, C.-K. Tsung, Y. Yamada, P. Yang and G. A. Somorjai, *Nature Materials*, 2009, **8**, 126-131.
12. C. M. Y. Yeung, K. M. K. Yu, Q. J. Fu, D. Thompsett, M. I. Petch and S. C. Tsang, *Journal of the American Chemical Society*, 2005, **127**, 18010-18011.
13. C. M. Y. Yeung and S. C. Tsang, *Journal of Physical Chemistry C*, 2009, **113**, 6074-6084.

14. M. Cargnello, J. J. D. Jaén, J. C. H. Garrido, K. Bakhmutsky, T. Montini, J. J. C. Gámez, R. J. Gorte and P. Fornasiero, *Science Magazine*, 2012, **337**, 713-717.
15. M. Cargnello, N. L. Wieder, T. Montini, R. J. Gorte and P. Fornasiero, *Journal of the American Chemical Society*, 2010, **132**, 1402-1409.
16. K. Kishita, H. Sakai, H. Tanaka, H. Saka, K. Kuroda, M. Sakamoto, A. Watabe and T. Kamino, *Journal of Electron Microscopy*, 2009, **58**, 331-339.
17. A. T. DeLaRiva, T. W. Hansen, S. R. Challa and A. K. Datye, *Journal of Catalysis*, 2013, **308**, 291-305.